Ultrafiltration of Single-Chain Polymer Nanoparticles through Nanopores and Nanoslits

José A. Pomposo,[a,b,c]* Jon Rubio-Cervilla,[a] Edurne Gonzalez,[a] Angel J. Moreno,[a,d] Arantxa Arbe,[a] and Juan Colmenero[a,b,d]

[a] *Centro de Física de Materiales (CSIC, UPV/EHU) and Materials Physics Center MPC, Paseo Manuel de Lardizabal 5, E-20018 San Sebastián, Spain.*

[b] *Departamento de Física de Materiales, Universidad del País Vasco (UPV/EHU), Apartado 1072, E-20800 San Sebastián, Spain*

[c] *IKERBASQUE - Basque Foundation for Science, María Díaz de Haro 3, E-48013 Bilbao, Spain*

[d] *Donostia International Physics Center (DIPC), Paseo Manuel de Lardizabal 4, E-20018 San Sebastián, Spain*

* E-mail: Josetxo.pomposo@ehu.eus

ABSTRACT: Understanding the translocation of soft, conformable single-chain polymer nanoparticles (SCNPs) with intricate topology through nanopores and nanoslits is of great interest for several potential applications, including modern single-molecule analytical characterization methods. This work focus on the ultrafiltration of an elastic SCNP of size R through a cylindrical pore of diameter $D << R$ or a rectangular slit of width $H << R$ under an elongational flow field. Concerning SCNP ultrafiltration through nanopores of different diameter, we find a scaling law in qualitative agreement with recent results concerning the ability of soft conformable nanoparticles to translocate through pores at least tenfold smaller in size. Moreover, SCNP ultrafiltration through rectangular nanoslits provides a simple way to determine the elasticity parameter of a real SCNP based on its experimentally determined minimum slit width for effective ultrafiltration.

1. Introduction

Understanding the translocation of macromolecules with different topologies through confinement geometries such as a cylindrical pore of diameter *D* or a rectangular slit of width *H* both smaller than the macromolecular size, *R*, (*i.e.*, ultrafiltration regime) is of great interest for both theoretical and practical point of views.[1-9] From an application perspective, understanding how confinement alters the conformation of topological complex polymers is of interest for increasing our comprehension of several biological processes such as endocytosis, extravasation or renal filtration,[9,10] to improve new polymeric drug delivery systems,[11,12] and for the development of innovative nanoanalytical devices,[13] to name only a few relevant examples. Complementary, extensive theoretical efforts have been carried out to predict scaling regimes of non-charged chains with complex topologies in nanochannel and nanoslit geometries,[1-6] as well as the corresponding critical flux rates for ultrafiltration under an elongational flow field[14] since the successive works by Peterlin,[15] Casassa and Tagami,[16] de Gennes,[17] Pincus,[18] and Daoudi and Brochard[19] related to the translocation of a (neutral) flexible linear polymer chain through a small cylindrical pore under a specific flow field.

In addition to the classical and relevant problem of ultrafiltration of linear polymers through nanopores, other more complex scenarios involving translocation of intricate chain topologies such as those displayed by randomly branched[2-5,20] and star[2,6,21] polymers have also been theoretically addressed. In particular, the conformational properties of macromolecules under confinement and the critical flow rate for ultrafiltration have been the subject of a variety of theoretical approaches (*e.g.*, Flory-type treatment of the free energy under confinement,[1,22] "blob" model of confined polymers,[1] balance of hydrodynamic drag and confinement forces on an individual

blob[14]). When compared to theoretical achievements, however, experimental progress in this field has been significantly delayed due to the difficulty in preparation of uniform polymers with complex topologies and well-defined ultrafiltration membranes as well as to guarantee a complete elongational flux at nanopore entrance, although significant advances have been observed in recent years.[4] Interestingly enough, a unified description of transportation of polymer chains with different topologies (linear, branched, star) through a small cylindrical pore has been recently established by Wu and Li,[14] paving the way to consider the case of even more complex topologies, such as those displayed by so-called single-chain polymer nanoparticles (SCNPs) (*i.e.*, individual intrachain cross-linked polymer chains).[23] In recent years, the self-folding of an individual linear polymer chain (precursor) to a SCNP *via* intrachain covalent, noncovalent or dynamic covalent bonds[24-33] has attracted significant interest due to the potential applications of these nano-objects with complex topology in nanomedicine,[34-37] biosensing,[38-40] and catalysis,[41-45] among other different fields.[23] In this sense, understanding the translocation of a SCNP through confinement geometries and estimating the critical flow rate of SCNP ultrafiltration is of great interest for several potential applications, as well as to establish reliable single-molecule analytical characterization methods of these complex nano-objects.

Recently, we have introduced a simple theoretical model of covalent-bonded SCNPs by considering these intrachain cross-linked nano-objects as elastic unimolecular networks with effective elasticity parameter K.[46] The elastic SCNP model allows one to understand the effect of precursor polymerization degree (N) and cross-linking degree (x) or elasticity characteristics ($K \propto x$) on SCNP size (R), both in solvents of different quality and on substrates of different surface energy. Moreover, the elastic SCNP model has been validated by comparison of model predictions with

experimental data from a variety of covalent-bonded SCNP systems either under good solvent conditions at high dilution[47,48] or deposited on different solid substrates.[49-54]

Herein we adopt the elastic SCNP model to investigate the ultrafiltration of (non-charged) SCNPs in good solvent through a cylindrical pore of diameter $D << R$ or a rectangular slit of width $H << R$ under an elongational flow field. We focus on determining the SCNP conformational properties and change in free energy upon confinement, to locate the passing/clogging transition of SCNPs through nanopores and nanoslits, and to estimate the critical flow rate of SCNP ultrafiltration through nanopores and nanoslits. More elaborated theoretical treatments such as those concerning SCNP translocation dynamics, involving configurational entropy considerations[55] and non-equilibrium dynamics,[56] are outside of the scope of this work. Similarly, we do not consider here neither SCNPs under three-dimensional confinement (*e.g.*, SCNPs inside spherical nanocavities)[3] nor ultrafiltration of SCNPs prepared from semiflexible polymer precursors.[57,58]

The article is organized as follows. In section 2 we first summarize the general model of elastic SCNPs without dimensional confinement and then we apply the model to the case of ultrafiltration of SCNPs through nanopores and nanoslits. Next, scaling expressions for SCNP size under confinement, SCNP blob size, confinement free energy, minimum pore size / slit width for SCNP ultrafiltration and critical flow rate for SCNP translocation through nanopores and nanoslits are derived. A discussion of the main results obtained is provided in section 3 and, finally, the conclusions of the work are given in section 4.

2. Theoretical Section

2.1 Elastic Single-Chain Nanoparticles without Dimensional Confinement. *Size of Elastic Single-Chain Nanoparticles in Good Solvent Regime.*

We start our analysis by summarizing the general model of elastic SCNPs without any confinement effect (*e.g.*, under good solvent conditions at high dilution).[46] In the model, individual (neutral) SCNPs are assumed to be formed *via* intrachain covalent bonds from a flexible linear polymeric precursor of total number of monomers N containing two different monomers distributed randomly along the chain: reactive monomers of type A and unreactive monomers of type B. The number fraction of A monomers in the precursor is x. During SCNP formation (by assuming very high dilution) the A monomers of each individual chain are expected to dimerize to produce intramolecular cross-links of type A-A. Each resulting SCNP of size R can be regarded as an elastic unimolecular network composed of elastic strands connected by cross-links (see Figure 1A).

According to this simple model, the Flory-type free energy (F) of elastic SCNPs contains two contributions:[46] (i) an elastic free energy (F_{el}) arising from the presence of elastic strands connected by cross-links, and (ii) an excluded volume contribution (F_{ex}) from the balance of monomer-monomer and monomer-solvent interactions, such as

$$\frac{F(R)}{k_B T} \approx \frac{F_{el}(R)}{k_B T} + \frac{F_{ex}(R)}{k_B T} \qquad (1)$$

where k_B is the Boltzmann constant and T the absolute temperature. The elastic free energy is given by

$$\frac{F_{el}(R)}{k_B T} \approx \frac{R^2}{R_0^2} + KR^2 \qquad (2)$$

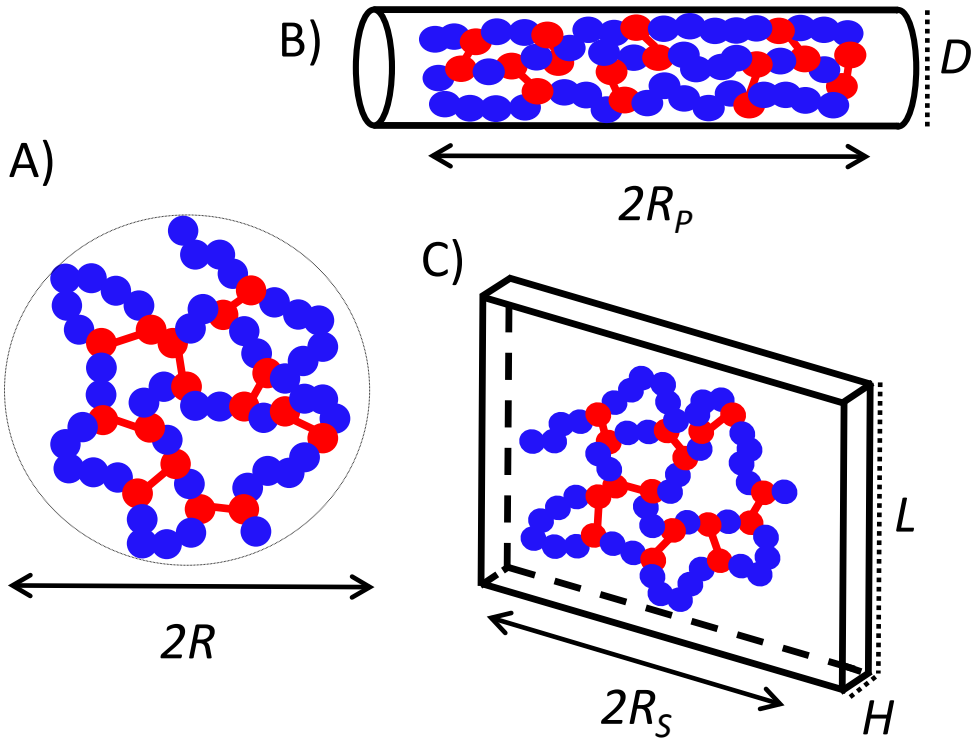

Figure 1. Schematic illustration of an elastic single-chain polymer nanoparticle (SCNP) regarded as a network of elastic strands (blue color) connected by cross-links (red color): (A) In a good solvent without dimensional confinement[46] (SCNP radius: R). (B) Under confinement in a cylindrical pore of diameter D (SCNP radius: R_P). (C) Under confinement in a rectangular slit of cross-sectional area $H \times L$ (SCNP radius: R_S).

where $R_0 \approx aN^{1/2}$, a is related to the monomeric segment length, K is a elasticity parameter proportional to x such as $K = Ax$, and A is the corresponding proportionality constant. In the limit $x \rightarrow 0$ (*i.e.*, $K \rightarrow 0$) eq 2 reduces to the well-known Flory expression for a flexible linear polymer chain. On the other hand, for elastic SCNPs (*i.e.*, $K >> R_0^{-2}$) eq 2 becomes

$$\frac{F_{el}(R)}{k_B T} \approx KR^2 = AxR^2 \qquad (3)$$

When the model was compared to experimental data of real SCNPs in ref. 46, the assumption $K >> R_0^{-2}$ was found to be a very good approximation. As an example, for polystyrene (PS) SCNPs the value of *A* was estimated to be 47.6 nm^{-2}, so the condition $K = Ax > R_0^{-2}$ was met even in the limit of relatively low values of *N* and extremely low values of *x* (*e.g.*, for $N = 500$ and *x* as low as 0.025).[46] Under good solvent conditions, the excluded volume contribution to the free energy is given by

$$\frac{F_{ex}(R)}{k_B T} \approx \frac{N^2 a^3}{R^3} \qquad (4)$$

so the free energy of elastic SCNPs (eq. 1) becomes

$$\frac{F(R)}{k_B T} \approx KR^2 + \frac{N^2 a^3}{R^3} \qquad (5)$$

and the equilibrium configuration of the elastic SCNP without dimensional confinement, as obtained by minimizing eq 5 with respect to *R*, is given by

$$R \approx a^{3/5} K^{-1/5} N^{2/5} \qquad (6)$$

Eq. 6 was used to fit reliable experimental size data of PS SCNPs providing an average deviation between calculated and experimental data of only 4.2 %.[46]

2.2 Elastic Single-Chain Nanoparticles Confined in Cylindrical Pores. *Optimum Extension of an Elastic Single-Chain Nanoparticle Confined in a Nanopore.* Now, let us confine an elastic SCNP in good solvent regime into a narrow cylindrical pore with diameter $D << R$ (see Figure 1B). Consequently, the SCNP is stretched along the channel axis with the length $R_P > R$.

Since now the volume available to the confined SCNP is $\simeq D^2 R_P$, the free energy expression (eq 5) becomes

$$\frac{F(R_P)}{k_B T} \approx K R_P^2 + \frac{N^2 a^3}{D^2 R_P} \qquad (7)$$

and, after minimization, the equilibrium configuration of the confined SCNP is given by

$$R_P \approx a K^{-1/3} \left(\frac{N}{D} \right)^{2/3} \qquad (8)$$

For elastic SCNPs R_P is predicted to depend on the elasticity parameter, $K = Ax$, with a scaling exponent of -1/3 (≈ -0.33) (*i.e.*, R_P decreases upon increasing the intrachain cross-linking degree, *x*, and hence *K*) and the scaling exponent of R_P on *N* is 2/3 (≈ 0.67). For comparison, the scaling exponent of R_P on *N* is 5/6 (≈ 0.83) for randomly branched polymers and 1 for linear chains.[20]

Blob Size of an Elastic Single-Chain Nanoparticle Confined in a Nanopore. Complementary, the elastic SCNP confined in the nanopore can be viewed as a string of blobs with size ξ_P and *g* segments each, such as the volume fraction ϕ is

$$\phi \approx \frac{N a^3}{D^2 R_P} \approx \frac{g a^3}{\xi_P^3} \qquad (9)$$

Inside each blob (good solvent conditions, no confinement inside the blob) we can assume

$$\xi_P \approx a^{3/5} K^{-1/5} g^{2/5} \qquad (10)$$

Hence, by combining eq 8, 9 and 10 we obtain the blob size of an elastic SCNP confined in a cylindrical nanopore of diameter *D* such as

$$\xi_P \approx a^{-1} K^{1/3} D^{8/3} N^{-2/3} \qquad (11)$$

Eq. 11 will be used below to determine the critical flow rate (J_P^c) for translocation of an elastic SCNP through a cylindrical pore under an elongational flow field.

Free Energy of SCNP Confinement in a Nanopore. The change in free energy upon SCNP confinement in a nanopore (F_P^c) can be estimated from[3]

$$\frac{F_P^c}{k_B T} \approx \frac{D^2 R_P}{\xi_P^3} \qquad (12)$$

So from eq 6, 8 and 11 we obtain

$$\frac{F_P^c}{k_B T} \approx K^{-4/3} \left(\frac{a}{D}\right)^4 \left(\frac{N}{D}\right)^{8/3} \qquad (13a)$$

$$\frac{F_P^c}{k_B T} \approx \left(\frac{R}{D}\right)^{20/3} \qquad (13b)$$

Instead of the exponent 20/3 (≈ 6.67), for branched polymers and linear chains in nanopores the scaling exponent of F_P^c on R / D is 8/3 (≈ 2.67) and 5/3 (≈ 1.67) respectively.[3]

Location of the Passing/Clogging Transition of an Elastic Single-Chain Nanoparticle in the D vs R Diagram. The minimum pore size (D_{min}) for translocation of an elastic SCNP through a long, cylindrical nanopore is obtained from the condition of the highest possible packing inside the pore, $\phi \approx \frac{Na^3}{D_{min}^2 R_P} = 1$, and from eq 8 it is given by

$$D_{min} \approx a^{3/2}(KN)^{1/4} \qquad (14)$$

Similar to the case of branched polymers discussed by Sakaue and Brochard-Wyart,[20] Eq 14 defines the passing / clogging transition for elastic SCNPs through a long, cylindrical nanopore: the SCNP cannot pass across a pore of diameter $D < D_{min}$.[59] For elastic SCNPs D_{min} scales with the elasticity parameter K with an exponent of 1/4 (= 0.25) (*i.e.*, D_{min} increases upon increasing K) and the scaling exponent of D_{min} on N is also 1/4. For comparison, the scaling exponent of D_{min} on N is 1/8 (= 0.125) for branched polymers and 0 (no dependence) for linear polymer chains.[20]

It is instructive to rewrite eq 14 in terms of the SCNP size out of the nanopore, R, so from eq 6 we obtain

$$D_{min} \approx a^{9/8}K^{3/8}R^{5/8} \qquad (15)$$

Determination of the Elasticity Parameter from Minimum Pore Size Measurements in Nanopores. According to eq 15, D_{min} is predicted to depend on the elasticity parameter K with a scaling exponent of 3/8 (≈ 0.38), which is a promising result in order to separate real SCNPs of the same size but different intrachain cross-linking degrees *via* filtration through long, cylindrical nanopores of track-etch membranes having different D values. Moreover, following Sakaue and Brochard-Wyart[20] one can envision an alternative way to determine D_{min} by tuning the channel cross-sectional size D in a soft elastomeric channel by applying a mechanical compressional force.[60] From a practical point of view, according to eq 14 and 15 the elasticity constant K of a SCNP of N monomers and size R could be determined from the experimentally determined value of D_{min} through

$$K = a^{-6} D_{min}^{4} N^{-1} \quad (16a)$$

$$K = a^{-3} D_{min}^{8/3} R^{-5/3} \quad (16b)$$

Critical Flow Rate for Elastic Single-Chain Nanoparticle Translocation through a Nanopore under an Elongational Flow Field. In addition to the conformational properties of elastic SCNPs confined in nanopores, the free energy of SCNP confinement, and the location of the passing/clogging transition in the *D* vs *R* diagram, the critical flow rate for translocation of an elastic SCNP through a cylindrical pore under an elongational flow field (J_P^c) is of great interest for practical applications. To obtain an expression for J_P^c, we follow here the methodology of Wu and coworkers,[4] which relies on the balance of confinement (f_c) and hydrodynamic (f_h) forces acting on an individual polymer blob of size ξ_P. The forces on the blob are given, to a first approximation, by[4]

$$f_c \approx \frac{k_B T}{\xi_P} \quad (17)$$

and

$$f_h \approx \frac{3\pi\eta\xi_P J}{D^2} \quad (18)$$

where η and *J* are the solvent viscosity and flow rate, respectively. By imposing the condition $f_c = f_h$, the critical flow rate is obtained such as[4]

$$J_P^c \approx \frac{k_B T}{3\pi\eta}\left(\frac{D}{\xi_P}\right)^2 \quad (19)$$

As pointed out by Wu and coworkers,[4,14] eq 19 should be valid without any prior consideration of the chain topology (linear, star, branched, etc.) relying exclusively on

the specific value of ξ_P for each topology. By taking the critical flow rate of flexible linear polymer chains as a reference ($J_P^{c_0} \approx \frac{k_B T}{3\pi\eta}$) eq 19 can be expressed as[4]

$$\frac{J_P^c}{J_P^{c_0}} \approx \left(\frac{D}{\xi_P} \right)^2 \qquad (20)$$

For elastic SCNPs, a useful expression for $\frac{J_P^c}{J_P^{c_0}}$ results by combining eq. 11 and 20 such as

$$\frac{J_P^c}{J_P^{c_0}} \approx a^2 K^{-2/3} D^{-10/3} N^{4/3} \qquad (21a)$$

$$\frac{J_P^c}{J_P^{c_0}} \approx \left(\frac{R}{D} \right)^{10/3} \qquad (21b)$$

Eq. 21 is valid only under confinement conditions. For comparison, instead of 10/3 (≈ 3.33) the scaling exponent for branched polymers is predicted to be 2/3 (≈ 0.67).[4,14]

2.3 Elastic Single-Chain Nanoparticles Confined in Rectangular Slits. *Optimum Extension of an Elastic SCNP Confined in a Nanoslit.* Now we turn our attention to the case of an elastic SCNP in good solvent regime confined in a slit of width $H << R$ and lateral dimension L (see Figure 1C). The volume available to the confined SCNP is $\simeq HR_S^2$ so the free energy expression (eq 5) becomes

$$\frac{F(R_S)}{k_B T} \approx K R_S^2 + \frac{N^2 a^3}{H R_S^2} \qquad (22)$$

and the optimum extension of an elastic SCNP confined in a nanoslit, R_S, is given by

$$R_S \approx a^{3/4} (KH)^{-1/4} N^{1/2} \qquad (23)$$

Blob Size of an Elastic Single-Chain Nanoparticle Confined in a Nanoslit. An elastic SCNP confined in a nanoslit can be viewed as a string of blobs with size ξ_S and *g* segments each, such as

$$\phi \approx \frac{Na^3}{HR_S^2} \approx \frac{ga^3}{\xi_S^3} \tag{24}$$

and from eq 6

$$\xi_S \approx a^{3/5} K^{-1/5} g^{2/5} \tag{25}$$

Hence, by combining eq 23-25 the blob size of an elastic SCNP confined in a nanoslit is given by the simple result

$$\xi_S \approx H \tag{26}$$

Free Energy of SCNP Confinement in a Nanoslit. The change in free energy upon SCNP confinement in a nanoslit (F_S^c) is given by[3]

$$\frac{F_S^c}{k_B T} \approx \frac{HR_S^2}{\xi_S^3} \tag{27}$$

So from eq 6, 23 and 26 we obtain

$$\frac{F_S^c}{k_B T} \approx a^{3/2} K^{-1/2} H^{-5/2} N \tag{28a}$$

$$\frac{F_S^c}{k_B T} \approx \left(\frac{R}{H}\right)^{5/2} \tag{28b}$$

Instead of the above exponent (5/2 = 2.5) for branched polymers and linear chains in a nanoslit the scaling exponent of F_P^c on R / H is predicted to be 2 and 5/3 ≈ 1.67, respectively.[3]

Minimum Pore Size for Elastic Single-Chain Nanoparticle Translocation through a Nanoslit. The minimum width (H_{min}) for translocation of

an elastic SCNP through a long, rectangular nanoslit is obtained from the condition of the highest possible packing inside the slit, $\phi \approx \frac{Na^3}{H_{min}R_S^2} = 1$, so from eq 23

$$H_{min} \approx a^3 K \qquad (29)$$

Eq 29 defines the passing / clogging transition for elastic SCNPs through a long, rectangular nanoslit,[61] which is predicted to be independent on N (and, hence, R). According to eq 29, for elastic SCNPs H_{min} is directly proportional to K, which opens the way to determine the value of K from the experimentally determined value of H_{min} by performing translocation experiments with long, rectangular nanoslits having different H values.

Critical Flow Rate for Elastic Single-Chain Nanoparticle Translocation through a Nanoslit under an Elongational Flow Field. The critical flow rate for translocation of an elastic SCNP through a rectangular slit under an elongational flow field (J_S^c) can be derived following the methodology reported by Wu and coworkers[4] by taking into account the cross-sectional area of the slit ($H \times L$). In this case, the critical flow rate is given by

$$J_S^c \approx \frac{k_B T}{3\pi\eta}\left(\frac{HL}{\xi_S^2}\right) \qquad (30)$$

By combining eq 26 and 28 we obtain the simple result

$$J_S^c \approx J_P^{c_0}\left(\frac{L}{H}\right) \qquad (31)$$

Eq. 31 is valid only under confinement conditions.

3. Results and Discussion

The model of elastic SCNPs described in section 2 allows one: *(i)* to analyze the conformational properties and free energy of confinement concerning elastic SCNPs of size R placed in a cylindrical pore of diameter $D << R$ or a rectangular slit of width $H << R$ and lateral size L (see Figure 1), *(ii)* to locate the passing/clogging transition of SCNPs through nanopores and nanoslits, and *(iii)* to estimate the critical flow rate for translocation of elastic SCNPs through these confinement geometries.

Summary of Scaling Laws for Single-Chain Nanoparticles in Nanopores and Nanoslits. A summary of the scaling expressions derived in section 2.2 and 2.3 for elastic SCNPs in nanopores and nanoslits is given in Table 1. For the sake of clarity, a is taken as unity both in Table 1 and in the following discussion. From a practical point of view, two magnitudes are of significant interest: (i) the minimum size for translocation of an elastic SCNP through a nanopore (D_{min}) or a nanoslit (H_{min}) and (ii) the critical flow rate for translocation of an elastic SCNP through a cylindrical pore (J_P^c) or a rectangular slit (J_S^c).

Table 1. Scaling laws for ultrafiltration of single-chain polymeric nanoparticles through nanopores and nanoslits[a]

Magnitude	SCNPs in Cylindrical Pores	SCNPs in Rectangular Slits
Lateral size, R_i	$R_P \approx K^{-1/3}\left(\frac{N}{D}\right)^{2/3}$	$R_S \approx (KH)^{-1/4} N^{1/2}$
Blob size, ξ_i	$\xi_P \approx K^{1/3} D^{8/3} N^{-2/3}$	$\xi_S \approx H$

Free energy of confinement, F_i^c	$\frac{F_P^c}{k_BT} \approx \left(\frac{R}{D}\right)^{20/3}$	$\frac{F_S^c}{k_BT} \approx \left(\frac{R}{H}\right)^{5/2}$
Minimum size, X_{min}	$D_{min} \approx K^{3/8} R^{5/8}$	$H_{min} \approx K$
Critical flow rate, J_i^c	$\frac{J_P^c}{J_P^{c_0}} \approx \left(\frac{R}{D}\right)^{10/3}$	$J_S^c \approx J_P^{c_0} \left(\frac{L}{H}\right)$

[a] For the sake of clarity, we use a = 1. D = Pore diameter. H = Slit width. L = Slit lateral size. R = SCNP size without dimensional confinement. N = SCNP total number of monomers. K = SCNP elasticity parameter (see text).

Passing/Clogging Transition for Single-Chain Nanoparticles through Nanopores. Figure 2 shows the location of the passing/clogging transition in a D vs R diagram for ultrafiltration of SCNPs with different values of the elasticity parameter K through nanopores under an elongational flow field. For comparison, we have also included in Figure 2 the predictions for the case of branched polymers ($D_{min} \approx b^{-3/10} R^{1/4}$, where b is the average number of monomers between consecutive branching points) and linear chains. For the latter case, D_{min} is only determined by the monomer size, a result well-known in the literature.[1] For branched polymers, D_{min} is predicted to grow with R but with a relatively small value of the scaling exponent (1/4 ≈ 0.25). It is worth of mention that for elastic SCNPs, D_{min} takes significantly higher values even at low K values than those of branched polymers and linear chains, and D_{min} grows upon increasing R and K according to $D_{min} \approx K^{3/8} R^{5/8}$ (see Table 1). For SCNPs, the scaling

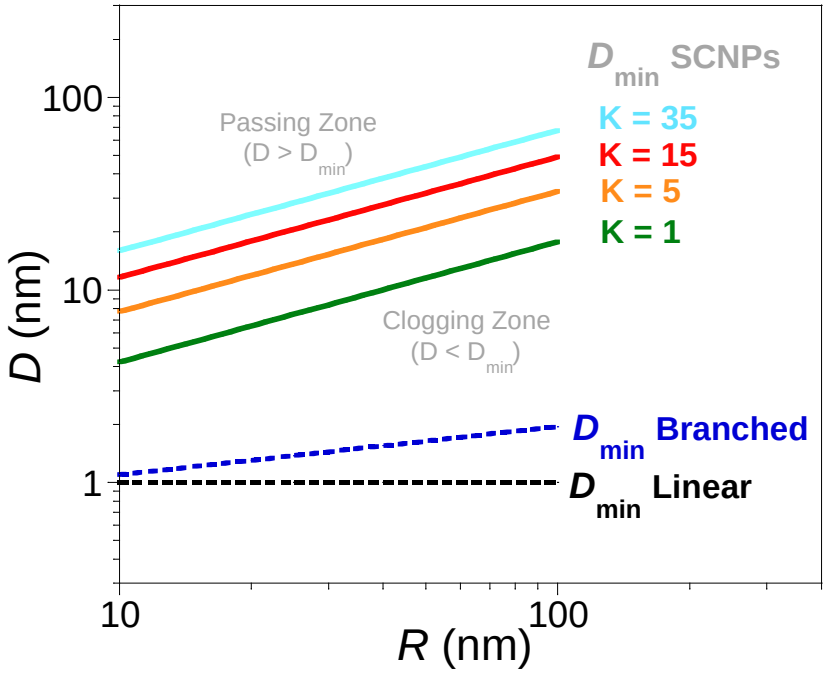

Figure 2. Location of the passing/clogging transition in the D vs R diagram of elastic single-chain nanoparticles through nanopores, as predicted from $D_{min} \approx K^{3/8} R^{5/8}$ for different values of the elasticity parameter K; randomly branched polymers, as calculated from $D_{min} \approx b^{-3/10} R^{1/4}$ with b = 5; and linear polymer chains.

exponent of D_{min} on R is predicted to take a value of 5/8 ≈ 0.63, which is much higher than that predicted for branched polymers. Moreover, the dependence of D_{min} on K (scaling exponent 3/8 ≈ 0.38) is very promising in order to potentially separate SCNPs of exactly the same size but different intrachain cross-linking degree (*i.e.*, K values) by means of experiments in nanopores. Hence, based on the scaling law $D_{min} \approx K^{3/8} R^{5/8}$, SCNPs of R = 20 nm will permeate through a nanopore of D = 20 nm only if K < 20 (*i.e.*, x < 0.4 by assuming a typical value of $A \approx 50$ nm^{-2}).[46] Similarly, SCNPs of R = 10 nm will permeate through nanopores of D = 10 nm only if K < 10 (x < 0.2 for $A \approx 50$ nm^{-2}) and so on. Interestingly enough, this prediction is in qualitative agreement with

recent results concerning the ability of soft conformable nanoparticles to translocate through pores at least tenfold smaller in size under relatively low hydrostatic pressures.[10] In such study, slightly cross-linked poly(*N*-isopropylacrylamide) (PNIPAM) particles with a diameter of 116 nm were found to pass across nanopores of D = 10 nm, whereas highly cross-linked PS beads with a diameter of 88 nm do not.[10] Based on the scaling expression $D_{min} \approx K^{3/8} R^{5/8}$, a slightly cross-linked particle of 116 nm in diameter is expected to pass across nanopores of D > 12.7 nm by assuming $K \approx 1$, whereas a highly cross-linked particle (let us assume $K \approx 35$) of 88 nm in diameter will only pass across nanopores of D > 40.4 nm.

Critical Flow Rate for Translocation through a Nanopore of Single-Chain Nanoparticles. Figure 3 illustrates the critical flow rate for translocation through a cylindrical pore (J_P^c) of elastic SCNPs, branched polymers and linear chains as a function of the R / D ratio. Data are normalized by the critical flow rate of linear polymers ($J_P^{c_0}$). When compared to linear chains ($\frac{J_P^c}{J_P^{c_0}} = 1$), higher values of relative critical flow rate for translocation through a cylindrical pore are predicted for branched polymers,[4] according to the scaling law $\frac{J_P^c}{J_P^{c_0}} \approx \left(\frac{R}{D} \right)^{2/3}$. It is worth of mention that the (fundamentally different from linear chains) R / D-dependence for branched polymers has been confirmed by Wu and coworkers[5] *via* ultrafiltration experiments, although the experimental scaling exponent of J_P^c / $J_P^{c_0}$ on R / D for branched polymers is ≃ 2.1 instead of 2/3 (≈ 0.67). For elastic SCNPs, a stronger dependence of J_P^c / $J_P^{c_0}$ on R / D is predicted than that corresponding to branched polymers, with a theoretical exponent of 10/3 (≈ 3.33).

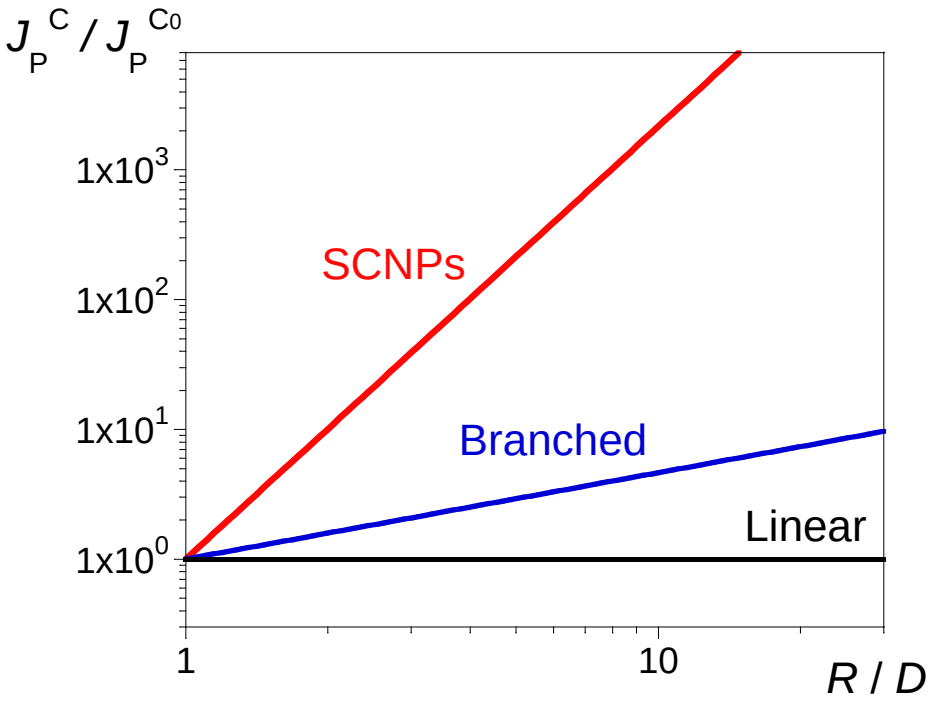

Figure 3. Relative critical flow rate ($J_P^c / J_P^{c_0}$) for translocation through a cylindrical pore of elastic single-chain nanoparticles, as predicted from $\frac{J_P^c}{J_P^{c_0}} \approx \left(\frac{R}{D}\right)^{10/3}$; branched polymers, as calculated from $\frac{J_P^c}{J_P^{c_0}} \approx \left(\frac{R}{D}\right)^{2/3}$; and linear chains.

Effect of Elasticity on the Critical Flow Rate for Translocation of Single-Chain Nanoparticles through a Cylindrical Pore. Concerning the experimental possibility to separate SCNPs of identical value of *N* but different values of *K* (and *x*) through a nanopore of diameter *D* based on differences in critical flow rate for translocation, we can estimate for this specific case how J_P^c will change upon increasing *K* from eq 21a, such as $\frac{J_P^c(K)}{J_P^c(K=1)} \approx K^{-2/3}$. Accordingly, the $\frac{J_P^c(K)}{J_P^c(K=1)}$ ratio for elastic SCNPs of identical value of *N* is expected to decrease from 1 to 0.09 on

increasing the elasticity parameter from $K = 1$ to $K = 35$, paving the way to the potential separation of SCNPs prepared from the same precursor (same value of N) but with different degrees of intrachain cross-linking (different values of x and, hence, K) by changing progressively the flow rate during ultrafiltration experiments.

Passing/Clogging Transition for Single-Chain Nanoparticles through Nanoslits. Concerning elastic SCNPs in nanoslits (see Figure 1C), Figure 4 shows the location of the passing/clogging transition in a H vs R diagram for elastic SCNPs having different values of the elasticity parameter K. In this case, H_{min} is predicted to depend *exclusively* on the elasticity parameter K (*i.e.*, no dependence on SCNP size). Consequently, experiments in nanoslits with different width values could provide a

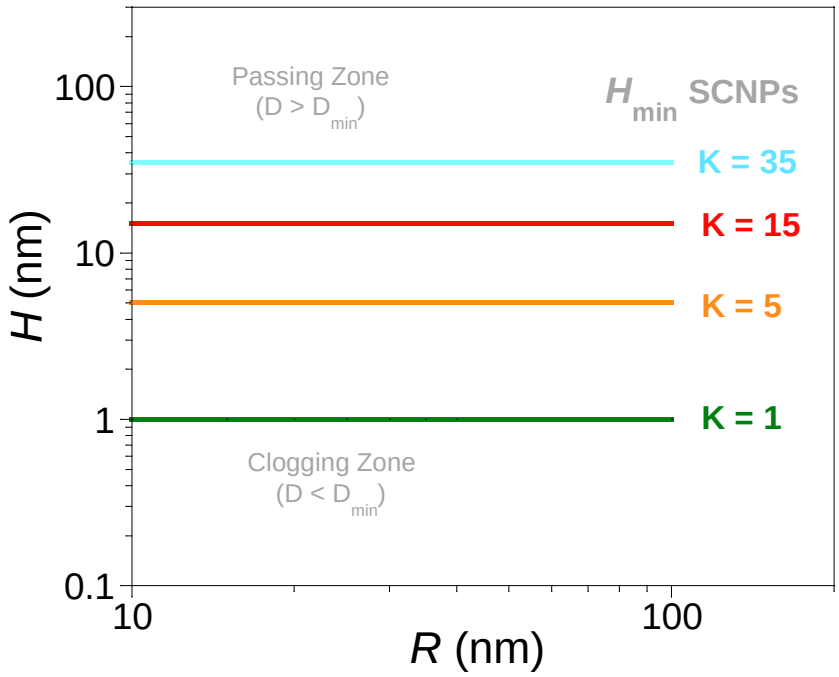

Figure 4. Location of the passing/clogging transition in the H vs R diagram of elastic single-chain nanoparticles of $R \geq H$ through nanoslits, as predicted from $H_{min} \approx K$ for different values of the elasticity parameter K.

simple way to estimate the value of K for real SCNPs based on the experimentally determined H_{min} value.

Critical Flow Rate for Translocation through a Nanoslit of Single-Chain Nanoparticles. For elastic SCNPs J_S^c (see Table 1) is predicted to be proportional to the L / H ratio but independent of K, N or R (taking into account that SCNP translocation through the nanoslit is only expected for $H > H_{min}$ as described above). Consequently, no information about the magnitude of K would be extracted from J_S^c measurements in experiments of SCNP translocation through nanoslits.

Comparison of Free Energy of Confinement for SCNPs in Nanopores and Nanoslits. Figure 5 illustrates the change in free energy upon confinement of an elastic SCNP of size R in a nanopore of size D (Figure 5A) or a nanoslit of width H (Figure 5B). The predictions for branched polymers and linear chains are also included

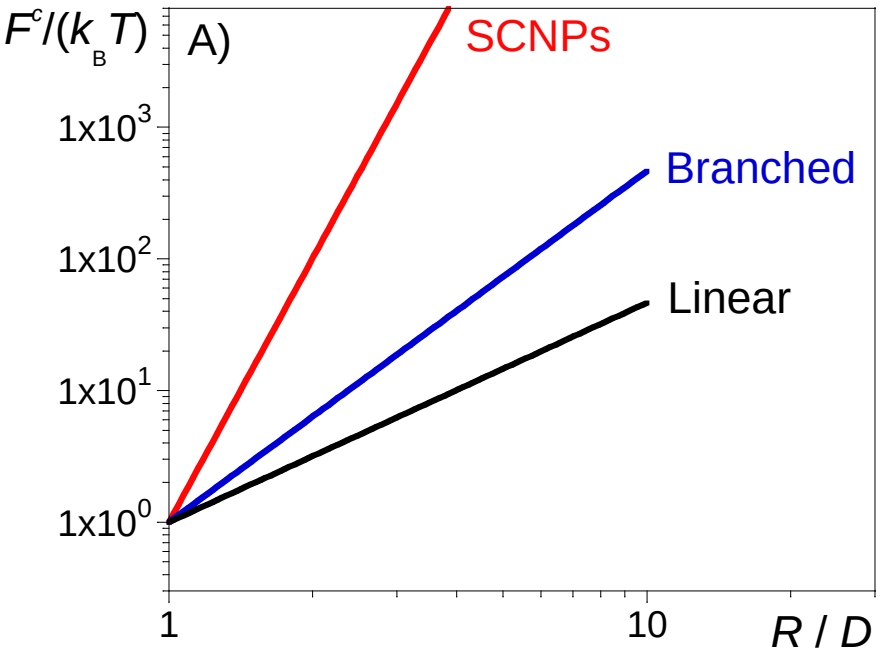

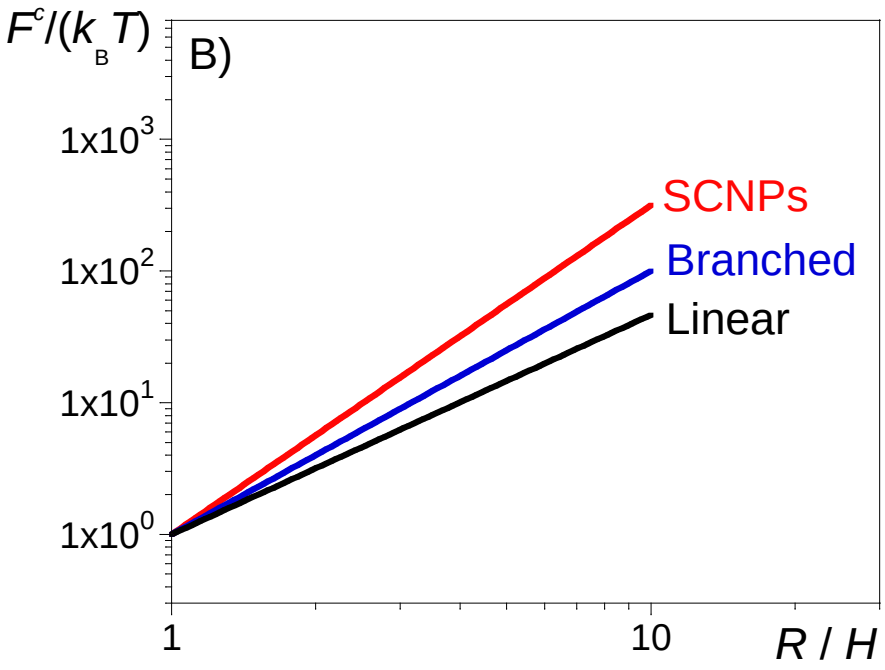

Figure 5. Free energy of confinement of elastic single-chain nanoparticles, branched polymers and linear chains, all of identical size *R*, in: A) Nanopores of different diameter *D*. B) Nanoslits of different width *H* (see text for details).

for comparison. As can be seen in Figure 5A, the penalty in free energy to confine an elastic SCNP in a nanopore of diameter *D* is significantly higher than that corresponding to the confinement of a flexible linear chain or a randomly branched polymer, all of them of identical size *R*. In the case of nanoslit confinement, the differences in free energy of confinement between the different polymer topologies are lower (Figure 5B). It is worth of mention that the free energy of confinement for a chain in a nanopore obeys the same scaling law than that for a chain in a nanoslit.[3] The differences observed for SCNPs and branched polymers in nanopores *vs.* nanoslits can be attributed to the stronger 1D-confinement imposed by nanopores to those intricate polymeric topologies when compared to 2D-confinement by nanoslits.[3]

4. Conclusions

In this work, we have focused on the ultrafiltration of a soft, conformable single-chain polymer nanoparticle of size R through a cylindrical pore of diameter $D << R$ or a rectangular slit of width $H << R$ under an elongational flow field and, more specifically: *(i)* to determine the SCNP conformational properties and change in free energy upon confinement, *(ii)* to locate the passing/clogging transition of SCNPs through nanopores and nanoslits, and *(iii)* to estimate the critical flow rate of SCNP ultrafiltration through these confinement geometries. Hence, we have derived useful scaling expressions concerning the SCNP size under confinement, blob size, free energy of confinement, minimum pore size / slit width for SCNP ultrafiltration and critical flow rate for SCNP translocation through nanopores and nanoslits.

Concerning the scaling expressions for SCNP ultrafiltration through cylindrical pores, we have found: *(i)* a scaling law for minimum pore size ($D_{min} \approx K^{3/8} R^{5/8}$) in qualitative agreement with recent results concerning the ability of soft conformable nanoparticles to translocate through pores at least tenfold smaller in size, *(ii)* a scaling law for the critical flow rate for SCNP translocation through nanopores ($J_P^c \approx J_P^{c_0} \left(\frac{R}{D} \right)^{10/3}$) with an exponent (10/3 ≈ 3.33) much higher than that experimentally found for hyperbranched polymers (≃ 2.1), and *(iii)* the possibility to separate SCNPs with the same molecular weight but very different intrachain cross-linking degree / elasticity characteristics by changing progressively the flow rate during nanopore ultrafiltration experiments, according to the ratio: $\frac{J_P^c(K)}{J_P^c(K=1)} \approx K^{-2/3}$.

Referred to the scaling expressions for SCNP ultrafiltration through rectangular slits we have found: *(i)* a very simple result for minimum slit width ($H_{min} \approx K$) providing an attractive way to estimate the *K* value of a real SCNP based on its experimentally determined H_{min} value, and *(ii)* a scaling law for the critical flow rate for SCNP translocation through nanoslits ($J_S^c \approx J_P^{c_0}\left(\frac{L}{H}\right)$) suggesting that no information about the magnitude of *K* would be extracted from J_S^c measurements in experiments of SCNP translocation through nanoslits.

Acknowledgements

Financial support by the Spanish Ministry "Ministerio de Economia y Competitividad", MAT2015-63704-P (MINECO / FEDER, UE), the Basque Government, IT-654-13, and the Gipuzkoako Foru Aldundia, Programa Red Gipuzkoana de Ciencia, Tecnología e Innovación 2017 (RED 101/17), is acknowledged. J.R.-C. is grateful to the Materials Physics Center MPC for his predoctoral grant. E. G. received funding from the "Fellows Gipuzkoa" fellowship of the Gipuzkoako Foru Aldundia.

References and notes

[1] P.-G. de Gennes, *Scaling Concepts in Polymer Physics*; Cornell University Press: Ithaca, NY, 1979.

[2] P.-G. de Gennes, Adv. Polym. Sci. 138 (1999) 91.

[3] T. Sakaue, E. Raphaël, Macromolecules 39 (2006) 2621.

[4] L. Li, Q. Chen, F. Jin, C. Wu, Polymer 67 (2015) A1.

[5] L. Li, Q. Chen, W. He, C. Wu, Macromolecules 45 (2012) 7583.

[6] H. Ge, S. Pispas, C. Wu, Polym. Chem. 2 (2011) 1071.

[7] Y. Wang, I. Teraoka, F. Y. Hansen, G. H. Peters, O. Hassager, Macromolecules 44 (2010) 403.

[8] F. Jin, C. Wu, Phys. Rev. Lett. 96 (2006) 237801.

[9] J. Cai, Y. Yue, D. Rui, Y. Zhang, S. Liu, C. Wu, Macromolecules 44 (2011) 2050.

[10] G. R. Hendrickson, L. A. Lyon, Angew. Chem. Int. Ed. 49 (2010) 2193.

[11] M. E. Fox, F. C. Szoka, J. M. J. Fréchet, Acc. Chem. Res. 42 (2009) 1141.

[12] D. P. Yang, M. N. N. L. Oo, G. R. Deen, Z. Li, X. J. Loh, Macromol. Rapid Commun. 38 (2017) 1700410.

[13] Y. Zhang, W. Reisner, Nanotechnology 26 (2015) 455301.

[14] C. Wu, L. Li, Polymer 54 (2013) 1463.

[15] A. Peterlin, Pure Appl. Chem. 12 (1966) 563.

[16] E. F. Casassa, Y. Tagami, Macromolecules 2 (1969) 14.

[17] P.-G. de Gennes, J. Chem. Phys. 60 (1974) 5030.

[18] P. Pincus, Macromolecules 9 (1976) 386.

[19] S. Daoudi, F. Brochard, Macromolecules 11 (1978) 751.

[20] T. Sakaue, F. Brochard-Wyart, ACS Macro Lett. 3 (2014) 194.

[21] F. Brochard-Wyart, P.-G. de Gennes, C. R. Acad. Sci., Ser. IIb: Mec., Phys., Chim., Astron. 323 (1996) 473.

[22] Flory, P. J. *Principles of Polymer Chemistry*; Cornell University Press: New York, 1953.

[23] *Single-Chain Polymer Nanoparticles: Synthesis, Characterization, Simulations and Applications*; Ed.: Pomposo, J. A.; Wiley-VCH: Weinheim, 2017.

[24] S. Mavila, O. Eivgi, I. Berkovich, N. G. Lemcoff, Chem. Rev. 116 (2016) 878.

[25] A. M. Hanlon, C. K. Lyon, E. B. Berda, Macromolecules 49 (2016) 2.

[26] O. Altintas, C. Barner-Kowollik, Macromol. Rapid Commun. 37 (2016) 29.

[27] M. Gonzalez-Burgos, A. Latorre-Sanchez, J. A. Pomposo, Chem. Soc. Rev. 44 (2015) 6122.

[28] C. K. Lyon, A. Prasher, A. M. Hanlon, B. T. Tuten, C. A. Tooley, P. G. Frank, E. B. Berda, Polym. Chem. 6 (2015) 181.

[29] A. Sanchez-Sanchez, J. A. Pomposo, Part. Part. Syst. Charact. 31 (2014) 11.

[30] A. Müge, H. Elisa, E. W. Meijer, A. R. A. Palmans, In *Sequence-Controlled Polymers: Synthesis, Self-Assembly, and Properties*; American Chemical Society: 2014; Vol. 1170, p. 313.

[31] A. Sanchez-Sanchez, I. Perez-Baena, J. A. Pomposo, Molecules 18 (2013) 3339.

[32] O. Altintas, C. Barner-Kowollik, Macromol. Rapid Commun. 33 (2012) 958.

[33] M. Aiertza, I. Odriozola, G. Cabañero, H.-J. Grande, I. Loinaz, Cell. Mol. Life Sci. 69 (2012) 337.

[34] Y. Bai, H. Xing, G. A. Vincil, J. Lee, E. J. Henderson, Y. Lu, N. G. Lemcoff, S. C. Zimmerman, Chem. Sci. 5 (2014) 2862.

[35] A. Sanchez-Sanchez, S. Akbari, A. J. Moreno, F. Lo Verso, A. Arbe, J. Colmenero, J. A. Pomposo, Macromol. Rapid Commun. 34 (2013) 1681.

[36] I. Perez-Baena, I. Loinaz, D. Padro, I. Garcia, H. J. Grande, I. Odriozola, J. Mater. Chem. 20 (2010) 6916.

[37] S. K. Hamilton, E. Harth, ACS Nano 3 (2009) 402.

[38] J. De-La-Cuesta, E. González, J. A. Pomposo, Molecules 22 (2017) 1819.

[39] A. Latorre-Sanchez, J. A. Pomposo, Chem. Commun. 51 (2015) 15736.

[40] M. A. J. Gillissen, I. K. Voets, E. W. Meijer, A. R. A. Palmans, Polym. Chem. 3 (2012) 3166.

[41] J. Rubio-Cervilla, E. González, J. A. Pomposo, Nanomaterials 7 (2017) 341.

[42] C. A. Tooley, S. Pazicni, E. B. Berda, Polym. Chem. 6 (2015) 7646.

[43] I. Perez-Baena, F. Barroso-Bujans, U. Gasser, A. Arbe, A. J. Moreno, J. Colmenero, J. A. Pomposo, ACS Macro Lett. 2 (2013) 775.

[44] E. Huerta, P. J. M. Stals, E. W. Meijer, A. R. A. Palmans, Angew. Chem., Int. Ed. 52 (2013) 2906.

[45] T. Terashima, T. Mes, T. F. A. De Greef, M. A. J. Gillissen, P. Besenius, A. R. A. Palmans, E. W. Meijer, J. Am. Chem. Soc. 133 (2011) 4742.

[46] J. De-La-Cuesta, E. González, A. J. Moreno, A. Arbe, J. Colmenero, J. A. Pomposo, Macromolecules 50 (2017) 6323.

[47] E. Harth, B. V. Horn, V. Y. Lee, D. S. Germack, C. P. Gonzales, R. D. Miller, C. J. Hawker, J. Am. Chem. Soc. 124 (2002) 8653.

[48] J. A. Pomposo, J. Rubio-Cervilla, A. J. Moreno, F. Lo Verso, P. Bacova, A. Arbe, J. Colmenero, Macromolecules 50 (2017) 1732.

[49] T. E. Dukette, M. E. Mackay, B. Van Horn, K. L. Wooley, E. Dockenmuller, M. Malkoch, C. J. Hawker, Nano Lett. 5 (2005) 1704.

[50] O. Altintas, J. Willenbacher, K. N. R. Wuest, K. K. Oehlenschlaeger, P. Krolla-Sidenstein, H. Gliemann, C. Barner-Kowollik, Macromolecules 46 (2013) 8092.

[51] P. Wang, H. Pu, M. Jin, J. Polym. Sci. Part A: Polym. Chem. 49 (2011) 5133.

[52] P. Wang, H. Pu, J. Ge, M. Jin, H. Pan, Z. Chang, D. Wan, Mater. Lett. 132 (2014) 102.

[53] I. Perez-Baena, I. Loinaz, D. Padro, I. Garcia, H. J. Grande, I. Odriozola, J. Mater. Chem. 20 (2010) 6916.

[54] A. Ruiz de Luzuriaga, I. Perez-Baena, S. Montes, I. Loinaz, I. Odriozola, I. García, J. A. Pomposo, Macromol. Symp. 296 (2010) 303.

[55] W. Sung, P. J. Park, Phys. Rev. Lett. 77 (1996) 783.

[56] J. Sarabadani, T. Ikonen, T. Ala-Nissila, J. Chem. Phys. 141 (2014) 214907.

[57] T. Sakaue, Macromolecules 40 (2007) 5206.

[58] A. J. Moreno, P. Bacova, F. Lo Verso, A. Arbe, J. Colmenero, J. A. Pomposo, J. Phys.: Condens. Matter 30 (2018) 034001.

[59] Eq. 20 is valid inasmuch the nanopore length is larger than $R_P(D_{min}) = (N/K)^{1/2}$.

[60] D. Huh, K. L. Mills, X. Zhu, M. A. Burns, M. D. Thouless, S. Takayama, Nat. Mater. 6 (2007) 424.

[61] Eq. 25 is valid inasmuch the slit perpendicular length is larger than $R_S(H_{min}) = (N/K)^{1/2}$.